Curvature of the Field Lines of Magnetic Braids

https://doi.org/10.31185/wjcm.VolX.IssX.XX

Murtadha Ali Rasheed(✉)
Education College for Pure Sciences, Wasit University, Iraq

Faik J H Mayah
College of Science, Wasit University, Iraq
faik@uowasit.edu.iq

Abstract— In this paper, we calculate the curvature numerically as a geometrical feature of the field lines of the magnetic braid that introduced by Antonia Wilmot-Smith and other new braid introduced in this work similar to that given by Wilmot-Smith but with four twisting regions are rotating one-by-one clockwise and anti-clockwise. The numerical calculation shows that the curvature of the field line of the new-version of the magnetic braid is much bigger than the curvature of the original model (Wilmot-Smith braid).

Keywords— Curvature, Magnetic Field, Field Line Mapping, Magnetic Braid.

1 Introduction

The magnetic field has the form of 3-dimensional vector field that is divergence - free ($\nabla . B = 0$). The divergence-free property reflects the fact that there is no source or sinks of magnetic field B, standing for the fact there are no magnetic monopoles [27]. This, however, does not mean that all magnetic field lines are closed. For instance, field lines can begin or end in magnetic null points [28]. In magnetohydrodynamics theory, the magnetic field often outlines the structure of different phenomena (e.g. sunspot or coronal loop) and it is reasonable to know the mapping which is produced by the magnetic field lines. The field lines are everywhere tangent to the magnetic field [29]. Facts collected under the title "magnetic topology" are mathematical consequence of the following system of the first-order ordinary differential equations for the magnetic field lines, see for instance [30].

$$\frac{\partial}{\partial t} X(x, t) = B(X(x, t), t), \tag{1a}$$

$$X(x_0, 0) = x_0 , \tag{1b}$$

where B= (B_x, B_y, B_z) is the magnetic field and it is known as a function of position. The solution of this system, i.e. $X(x, t)$ is a function of the initial position x parametrized by t.

These same properties apply to integral curves (or stream lines) found in other areas of physics, for example configuration space trajectories, stream lines or vortex lines.

Magnetic field lines are often closely related to physical structures, so that their topological properties can have direct physical significance. The field line mapping is a mathematical function that maps one domain in $D_1 \subseteq R^2$ to $D_2 \subseteq R^2$. There are many geometrical aspects one can measure them to investigate some properties of the field line mapping and the vector field. We will start by defining the vector field which is the first concept one should start to define the field line mapping by solving the system. The system is not easy to solve in most cases because the vector field itself is complex, and by complexity, we mean that the components of the vector field contain non - linear terms.

2 Vector Fields

A tangent vector to a manifold M^k subset of R^n at a point $x \in M^k$ is the velocity vector dy/dt to some curve $y = y(t)\ on\ M^k$. This curve is merely an image of some interval, or an image of the unit interval $I = [0,1] \subset R$ into M^k. This curve is describing by k differentiable functions $y^i = y^i(t)\,, i = 1..k$. The velocity vector $dy/dt\ \ at\ t = 0$ is described by the following real numbers

$$\frac{dy_U^1}{dt}, \frac{dy_U^2}{dt}, \dots, \frac{dy_U^k}{dt}$$

where U refers to the coordinate system about the point $y(0)$. If this point is also lying on another patch with coordinate system V, then the tangent vector can be defined in the following way [12].

Definition 2.1 A tangent vector at some point $x_\circ \in U \cap V \subset M^k$ is defined by the following

$$X_V^i = \sum_j \left(\left. \frac{\partial X_V^i}{\partial X_U^j} \right|_{x_\circ} \right) X_U^j$$

Let $f = f(x^1, x^2, \dots, x^k$ be a function defined on a manifold M^k. Now we will define the derivative of the function with respect to a vector W at some some point x_0.

$$W_{x_0}(f) = \sum_j \left. \frac{\partial f}{\partial x^j} \right|_{x_0} W^j$$

Definition 2.2 The tangent space to a manifold M^k at a point $x_0 \in M^k$ the real vector space that consists of all the tangent vectors to the manifold M^k at the point x_0. The following vectors

$$\frac{\partial}{\partial t^1}\Big|_{x_0}, \frac{\partial}{\partial t^2}\Big|_{x_0}, \dots, \frac{\partial}{\partial t^k}\Big|_{x_0}$$

where (t) is the coordinate system holding the point $x_\circ$.

A vector field $\boldsymbol{v}$ on a manifold R^k assigns a vector v to each point $x \in R^k$.

$$\boldsymbol{v} = \sum_j v^j(x_1, x_2, \dots, x_k)\frac{\partial}{\partial x^j}$$

Where $v^j(x_1, x_2, \dots, x_k)$ are differentiable functions.

The magnetic field or in general any force field can be modeled by representing (mathematically) the force field as a vector field.

3 Field Line Mappings

In order to understand the geometric aspects of the force field (in general the vector field) we might need to find the field line mapping that induced by the vector field. Solving the system (1) produce an equation that define the field lines (flow).

An example of such vector field, consider flow of water in the manifold R^3, so one can construct a family of maps

$$\varphi_S: R^3 \to R^3$$

Here φ_S , draw the path that trace the position of a molecule at $x_\circ$ when $s = 0$.

Lemma 3.1 If the flow is time independent, then

$$\varphi_t(\varphi_S(x)) = \varphi_{t+s}(x) = \varphi_S(\varphi_t(x))$$

and

$$\varphi_{-s}(\varphi_S(x)) = x$$

The following statement is an important theorem relating calculus to science. It allows us to find the integral line (stream line, or in general the field line mapping) by solving the system (1) [12].

Theorem 3.1 Let $\boldsymbol{w}$ be a vector field on an open set W of R^k.

$$\boldsymbol{w} : W \to R^k$$

$\boldsymbol{w}$ is associating to each point $p \in W$ a point$w(p)$ in R^k . Then for each x belong to W there is a curve α mapping an interval $(-a, a)$ into W

$$\alpha: (-a, a) \to W$$

such that for all $s \in (-a, a)$:

$$\frac{d\alpha(s)}{ds} = w(\alpha(s)) \; and \; \alpha(0) = x$$

There is W_x neighbourhood of the point x and a real number $\epsilon > 0$ and a mapping

$$\boldsymbol{\Phi}: W_x \times (-\epsilon\,, \epsilon\,) \to R^k$$

such that the curve $\phi_s(y) = \boldsymbol{\Phi}(\,y\,, s\,)$ satisfying the following differential equation.

$$\frac{\partial}{\partial s}\phi_s(y) = \boldsymbol{w}(\,\phi_s(y)\,) \tag{2}$$

This is defined one-parameter group of diffeomorphisms (flow) or field lines.

Any field in particular 3-dimensional vector field can be visualized by a set of magnetic field lines, that follow the direction of the field at each point. To construct the lines, we must measure the strength and direction of the magnetic field at the points of space. After that put at each location of point an arrow such that it is pointed in the direction of the local magnetic field with its magnitude proportional to the strength of the magnetic field. Trace the arrows by curves which forms a set of magnetic field lines. The direction of the magnetic field at any point is parallel to the direction of nearby field lines. In fluid flow, the stream lines are like the magnetic field lines are like streamlines in fluid flow, both represent a continuous distribution. Also, we can visualize these curves in different resolution by picking the number of lines of the vector field. Using the magnetic field lines as a representation of the field has a benefit because there are lots of laws in particular in electromagnetism are stated using simple concepts such as the " number" of field lines through a surface. These notions can be translated to their mathematical form. For instance, the number of field lines through a given surface is the surface integral of the magnetic field.

Example 3.1 (2-dimensional vector field) Consider the vector field given by

$$w = \frac{b_0}{l_0}\,(y\hat{\imath} + \alpha^2 x\hat{\jmath})$$

Let $b_0 = l_0 = 1$ and $\alpha = \frac{1}{\sqrt{2}}$ then the field line mapping can be produced by solving Eq 2.2, we get

$$\emptyset_1 = A\exp\left(\,\mathrm{s}\,/\,2^{\frac{1}{4}}\right) + B\exp\left(-\mathrm{s}\,/\,2^{\frac{1}{4}}\right)$$

$$\emptyset_2 = \frac{A\exp\left(\,\mathrm{s}\,/\,2^{\frac{1}{4}}\right) - B\exp\left(-\mathrm{s}\,/\,2^{\frac{1}{4}}\right)}{2^{\frac{1}{4}}}$$

The field line mapping $\Phi_s = \emptyset_1\hat{\imath} + \emptyset_2\,\hat{\jmath}$ with an arbitrary value of the constants A and B produced a picture given Figure 1 (right).

Example 3.2 (3-dimensional vector field) Consider the vector field given earlier

$$w = b_0\big(l_0 y\;\hat{\imath} + l_0 x\;\hat{\jmath} + \hat{k}\big)$$

Let $b_0 = l_0 = 1$ then the field line mapping can be obtained by the same way solving Eq. 2.2, We get

$$\emptyset_1 = A\exp(s) + B\exp(-s)$$
$$\emptyset_2 = A\exp(s) - B\exp(-s)$$
$$\emptyset_3 = s + C$$

The field line mapping $\Phi_s = \emptyset_1\,\hat{\imath} + \emptyset_2\hat{\jmath} + \emptyset_3\,\hat{k}$ with and arbitrary values of the constants A, B and C produced a picture given Figure 1 (left).

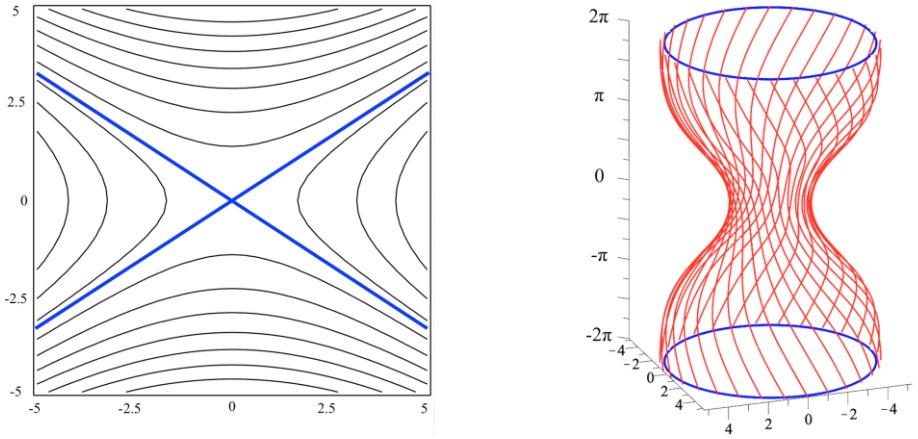

Figure 1 The field lines of the vector field given in Example 2.1 (left) and the vector field given in Example 2.2.

4 Magnetic Braids

4.1. Pigtail Braid

The pigtail braid can be constructed from three strands braided by six toroidal regions of flux. Each of these regions generates one over or under crossing of strands in the pigtail braid. The pigtail braid has been chosen because we expect that a field which is braided by random footpoint motions has on average the same number of over as under crossings. The pigtail braid has this property and in addition the pairwise linking I of the strands vanishes. The following is a mathematical formulation of the braids [4].

A braid β is a mathematical concept that represent some of string (or strand) or even field lines (in our context). The braid is described by using braid words (or operations) called σ_i, which are define the crossing of these paths [5].

The operations σ_i^{+1} and σ_i^{-1} on n paths, each oriented vertically from lower plane $p_l$to upper plane p_u , define a braid, where ± 1 refers to the direction of orientation.

Definition 4.4 [4] A braid β is defined as a product of σ_i^{+1} and σ_i^{-1}

$$\beta = \prod_i \sigma_i^s \ , where \ \ s = \pm 1$$

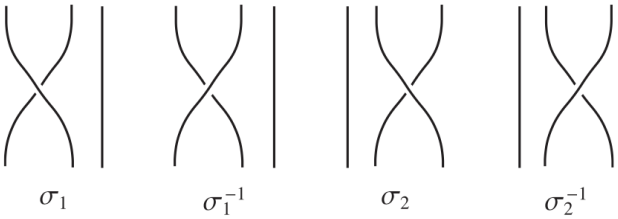

Figure 2 Braid word σ_1 , σ_1^{-1}, σ_2, σ_2^{-1} on 3 paths, Wikipedia.

The operator σ_i acts on the path i and $i+1$ by switching these paths such that the i^{th} path becomes above or down the $(i+1)^{th}$path as shown in Figure 2.

4.2 Braided Magnetic Field

Magnetic field is mathematically a vector field that demonstrate the interaction between the electric charge (current) and the magnetic materials. In particular, the force - free magnetic field is important in many astrophysical applications and the properties of such force - free fields can be considered the key to understanding energy release processes that heat the plasma and lead to dynamic events in the solar corona. The above group have investigated the properties of different relaxation procedures for determining force-free. In the case of a frozen - in field each field line moves with the plasma. These field lines will be continuously deformed by the flow $v(x\,,t)$ via the continuous flow field.

$$\frac{\partial B}{\partial t} - \nabla \times (v \times B) = 0 \qquad (3)$$

This means, for example, each closed field line will remain closed. We can see the utility of field line topology: preservation of the field line's topology by plasma motion, providing the plasma is a perfect conductor.

4.2.2 Wilmot-Smith's model

The solar photosphere rotates differentially , the rotation be faster at Sun's equator than at places with higher latitude . Due to the differential rotation, the magnetic field lines beneath the photosphere will be stretched and twisted . In addition to the differential rotation magnetic loops in the solar corona get braided due to turbulent motions at the solar surface or more precisely , the braiding come from the arbitrary footpoint motions at the photosphere . These processes are the motivation to consider models complex braided magnetic fields.

By analogy with the definition of the Dehn twist $re^{i\theta} \rightarrow re^{i(\theta+2\pi(r-1))}$ Wilmot - Smith and Priest (2007) used an example of a twisted magnetic flux tube. They took a constant magnetic field in z-direction with field strength $b_\circ$ between the planes $z = \pm H$ and added a toroidal region, by which a twist in the field is produced within $z = \pm L$ (i.e. the extent of the twist in the z-direction depend on the parameter L, also this mean that the azimuthal component of the magnetic field is localised). The width of the flux tube is dependent on a parameter a, and the ratio of I the toroidal field to the axial field governed by a parameter k.

Figure 3 shows some typical field lines of a flux tube of radius a. There is a localised twist within the tube in the region sandwiched by the planes

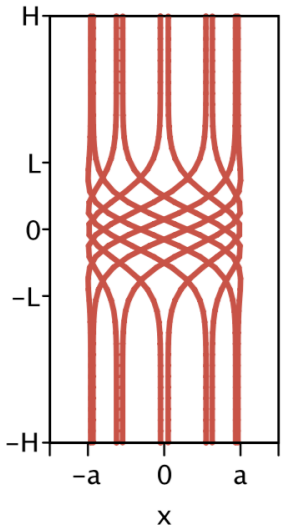

Figure 3 Some field lines starting from the level $z = -H$ and traced up the level $z = H$. Locally they rotate by π in the domain located between the planes $z = \pm L$, [10].

The magnetic field may be written in cylindrical coordinates as

$$B = b_\theta(r, b_0, k, a, L)\hat{\theta} + b_0\hat{z}$$
$$= 2b_0 k \frac{r}{a} exp\left(-\frac{r^2}{a^2} - \frac{z^2}{L^2}\right)\hat{\theta} + b_0\hat{z} \qquad (4)$$

This simple field configuration allows for a direct integration to find the equation of the field lines [2]. The equations, $R(r_0, \theta_0, s)$ of the field lines starting at the point $(r_0, \theta_0, z = 0)$ are given by

$$R = r_0 \qquad (5a)$$

$$\theta = 2b_0\, k\frac{r_0}{a}\; s \;\; exp\left(-\frac{{r_0}^2}{a^2}-\frac{{b_0}^2 s^2}{L^2}\right) \tag{5b}$$

$$Z = b_0 s \tag{5c}$$

These equations can be written in Cartesian coordinates as follows

$$X = -ysin(\theta) + xcos(\theta), \tag{6a}$$

$$Y = xsin\,(\theta) + y\cos(\theta), \tag{6b}$$

$$Z = b_\circ s \tag{6c}$$

where the angle of twisting θ is

$$\theta = \frac{\sqrt{\pi}Lk}{a}\;\; erf\left(\frac{b_\circ s}{L}\right)\exp\left(-\frac{r^2}{a^2}\right) \tag{7}$$

and $erf\left(\frac{b_\circ s}{L}\right)$ is the error function which is defined as

$$\mathrm{erf}(\xi) = \frac{2}{\sqrt{\pi}}\int_0^{\xi} e^{-u^2}du.$$

Now, the above Eqs. (2.6) are the coordinates of the field line mapping, which trace a twist in the magnetic field lines close to the origin . This mapping can be considered to be a building block for modelling braided magnetic fields [30].

The pigtail braid consists of three identical parts E, which we can define by:

$$E = F(F(x, y, z, x_c, y_c, z_c, 1); z\,, x_c, y_c, z_c, -1) \tag{8}$$

And $F: R^2 \to R^2$ is a mapping defined as following

$$F:\begin{pmatrix}x\\y\end{pmatrix} \to \begin{pmatrix}-(y-y_c)\sin\theta + (x-x_c)\cos\theta + x_c\\ (x-x_c)\sin\theta + (y-y_c)\cos\theta + y_c\end{pmatrix} \tag{9}$$

$$\theta = \pi k \exp\left(\frac{1}{2}\right)\frac{erf\left(\frac{s+z-z_c}{2}\right) - erf\left(\frac{z-z_c}{2}\right)}{\mathrm{erf}(2)} \times exp\left(-\frac{(x-x_c)^2+(y-y_c)^2}{2}\right) \tag{10}$$

The variables, z, x_c, y_c, z_c, k should take values.

Now, choose the point $(x_c, y_c, z_c) = (1, 0\,, z_{c1})$ to be the centre of twisting for the first level $(z = z_{c1} - 4)$ and choose $(x_c, y_c, z_c) = (1, 0\,, z_{c2})$ in the second level $(z = z_{c2} - 4)$ and compose the elementary part E three times to get the field line mapping labelled by E^3 which is modelled on the pigtail braid . To do this we can follow the three strands which start at$(2,0), (0,0), (-2,0)\; at\; z = -24$ and end up at $(2,0), (0,0), (-2,0)\; at\; z = +24$. Tracing this pigtail braid required evaluating it at each level by the parameters, where $0 \le s \le 48$. From the way we have constructed

the field line mapping these three strands form a pigtail and they have the following representation in braid theory.

$$\beta = \sigma_1\sigma_2^{-1}\sigma_1^{-1}\sigma_2\sigma_1\sigma_2^{-1}$$

The field line mapping given by:

$$\underbrace{E^n = E\left(E\left(\ldots\left(E(x,y)\right)\right)\right)}_{n-time} \tag{11}$$

which is induced by the following magnetic field:

$$B = \sum_{i=1}^{2n} B_{ci} + \hat{z} \tag{12}$$

where B_c defined by:

$$B_c = \sqrt{2}k \ \exp\left(\frac{-(x-x_c)^2-(y-y_c)^2}{2} - \frac{(z-z_c)^2}{4}\right) \times (-(y-y_c)\hat{x} + (x-x_c)\hat{y}). \tag{13}$$

Here(x_c, y_c, z_c) denotes the center of the rotation and k its orientation. That is each B_c, will represent a toroidal field region located in specific region determined by the triple(x_c, y_c, z_c). The following figure shows the two twisting region whose center at $(x_c, y_c) = (\pm 1, \pm 1)$ and they have opposite direction of rotations.

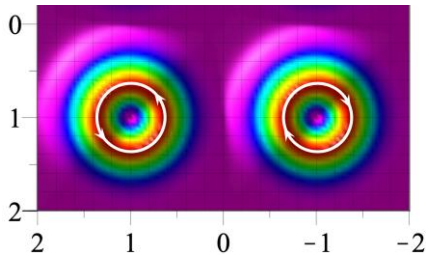

Figure 4 Two twisting region whose centre at $(x_c, y_c) = (\pm 1,1)$ defined by Eq. 13, with $c = 1,2$.

For our purposes $B_{ci}, i = 1 \ldots n$ correspond $c_i = ((-1)^{i+1}, 0, \tilde{z}_c + 8(i-1), (-1)^{i+1})and\ \tilde{z}_c$, can be chosen arbitrarily. Some of field line mapping in the first state of the braid are shown in the following figure.

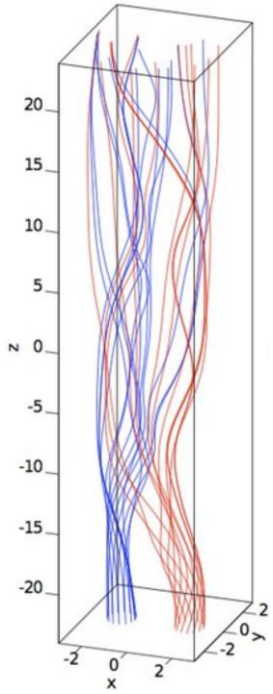

Figure 5 Typical field lines initiated from a points around two circles whose centres are the centres of the twisting regions (Wilmot-Smith 2007) [10].

4.2.2. Braids with quadratic twisting regions

Vector field $v: U \to R^3$, where U is a defined on R^3. In term of cartesian coordinates x^1, x^2, x^3

$$B = \left(\sum_{i=1}^{4} \sum_{j=1}^{2} B_i^j \frac{\partial}{\partial x^j} \right) + \frac{\partial}{\partial x^3} \tag{14}$$

where,

$$B_i^1 = -\sqrt{2}(-1)^i (x^2 - x_{ci}^2) e^{-\frac{1}{4}\left(x^3 - x_{ci}^3\right)^2} e^{-\frac{1}{2}\left(\left(x^1 - x_{ci}^1\right)^2 + \left(x^2 - x_{ci}^2\right)^2\right.} \tag{15}$$

$$B_i^2 = \sqrt{2}(-1)^i (x^1 - x_{ci}^1) e^{-\frac{1}{4}\left(x^3 - x_{ci}^3\right)^2} e^{-\frac{1}{2}\left(\left(x^1 - x_{ci}^1\right)^2 + \left(x^2 - x_{ci}^2\right)^2\right.} \tag{16}$$

It is easy to check that

$$\nabla . B = \frac{\partial}{\partial x^1} B_i^1 + \frac{\partial}{\partial x^2} B_i^1 + \frac{\partial}{\partial x^3}\ 1 = 0$$

which is indicate that this field is divergent-free.
This magnetic braid is modelled by Antonia Wilmot-Smith with two twisting regions appear in $x = \pm 1$ and used in many publications, recently used in [15].

We introduced this field in this manner for some reasons: the field is quit complex vie the four rotational regions which are take place in the above equations as the Gaussian terms , these regions have different direction of twisting according to the factor $(-1)^i$ and they have been distributed in the space as shown in the Figure 6.

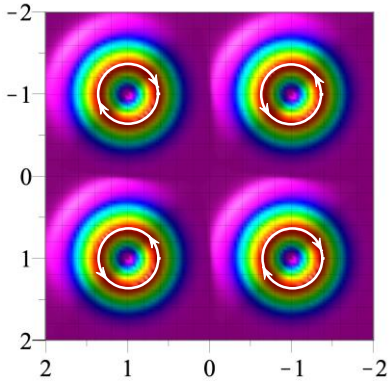

Figure 6 Four troroidal regions in the magnetic field that defined by Equation 15.

We have placed the toroidal centres at $(x_{ci}^1, x_{ci}^2, x_{ci}^3), i = 1,2,3,4$ each of which lies in one quarter in different level in x^3-direction. The integral curves of B are the solutions of the system of equation 2.1 that produce family of space curves that make a braid which is called a magnetic braid F define by a mapping $F: R^2 \rightarrow R^2$ as in Equation 2.9, θ is a twisting profile defined in the following way:

$$\theta = k\sqrt{\pi}\exp\left(\frac{-(x-x_c)^2-(y-y_c)^2}{2}\right)\frac{erf\left(\frac{s+z-z_c}{2}\right)-erf\left(\frac{z-z_c}{2}\right)}{erf(2)} \quad (17)$$

The profile of $\theta(s)$ has bell shape as shown below

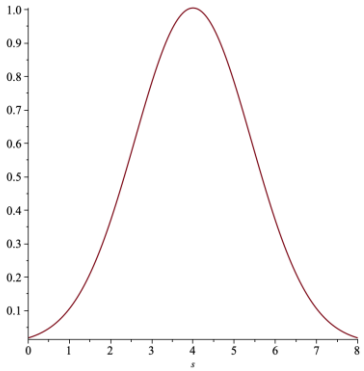

Figure 7 Profile of the gradient $\frac{d}{ds}\theta(s)$, the angle of rotation given by Eg. 17.

Now, choose the point $(x_c\,, y_c\,, z_c) = (\pm 1\,, \pm 1\,, s)$ to be the center of twists and s determine the level of twist in z-axis. The following Figure 8 shows some particular field lines in the domain initiated from four regions $(\pm 1 + \cos(t)\,, \pm 1 + \sin(t)), t \in [-\pi, \pi]$.

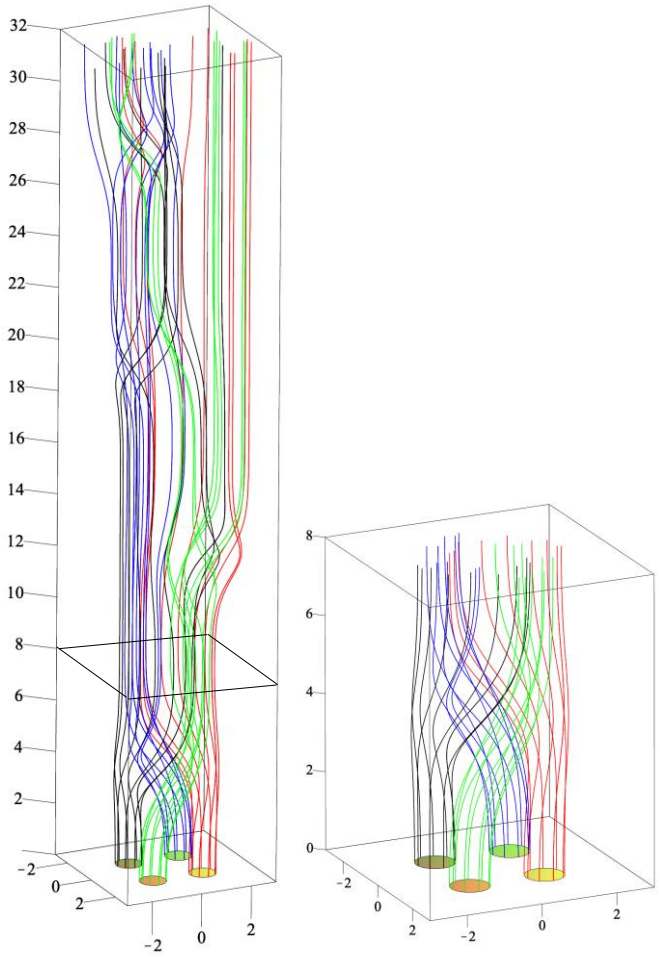

Figure 8 Some field lines that defined by Equation (9) initiated from four regions $(\pm 1 + cos(t), \pm 1 + sin(t)),\ t \in [-\pi, \pi]$.

As a test, Figure 9 shows how the mappings F and E deform a regular Cartesian grid. We note that the mesh is only deformed in a certain area around the centers (x_c, y_c) while further away the mesh remains undeformed. That means that even if we concatenate the mapping to obtain E^3 still have the mapping behave like the identity on the boundary.

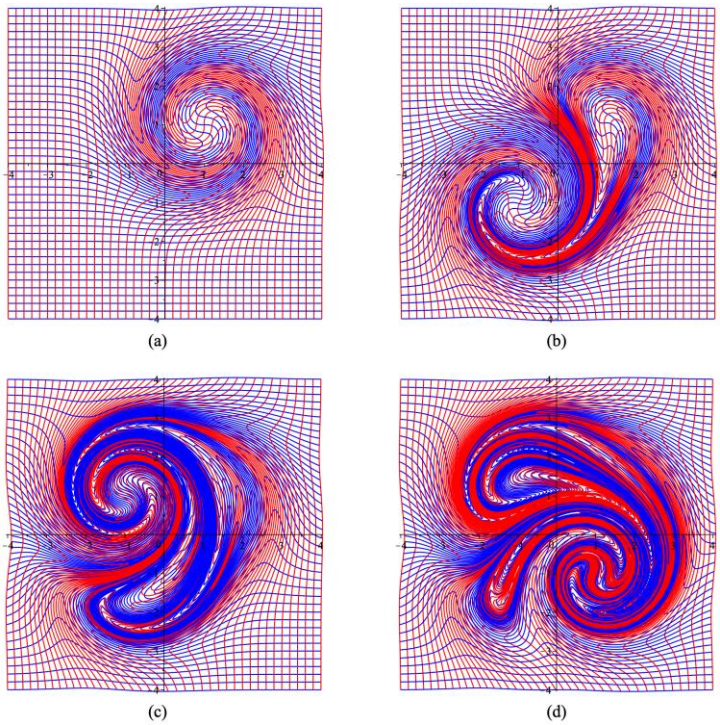

Figure 9 The figure illustrate the deformations of the mappings $F^{(n)} = F(F(\dots F(x, y; z, x\_c, y\_c, z\_c, k))$, *n times defined by Equation (9), where the resolution has been chosen is* 40^2.

5 Curvature of the Field Lines

Any parameterised curve $\gamma = \gamma(s)in\ R^3$ have a geometrical. Intuitively, the curvature is the amount by which a curve deviates from being a straight line. To calculate it, we associate to the curve $\gamma(s)$ its tangent $\gamma'(s)$ which is considered as velocity vector V with speed vector $\|V\|$. The are length parameter t is introduced by

$$\left(\frac{dt}{ds}\right)^2 = \|\gamma'(s)\|^2 = \|V\|^2, \quad t(s) = \int_0^s \|\gamma'(u)\| du$$

Then the unit tangent vector

$$t = \frac{d\gamma}{dt} = \gamma' \frac{ds}{dt} = \frac{V}{\|V\|}$$

This yield to

$$v = \|v\| t$$

The accretion is

$$a = v' = \|v\|'\, t + \|v\| \frac{dt}{ds} = \|v\|'\, t + \|v\|^2 \frac{dt}{ds}$$

The vector t and $\frac{d\boldsymbol{t}}{dt}$ are orthogonal because t has constant length. Moreover $\frac{d\boldsymbol{t}}{dt}$ and the curve $\gamma(s)$ are also orthogonal.

Definition 5.1. let $\frac{d\boldsymbol{t}}{dt} \neq 0$, the direction of an unit normal vector $\boldsymbol{n}(t)$ to the curve is called the principal normal and it is defined by

$$\frac{d\boldsymbol{t}}{ds} = k\,(t)\boldsymbol{n}(t) \tag{18}$$

where the function $k(t)$ is the curvature of $\gamma(t)$ at the value t.

Definition 5.2 Let $\gamma\colon (a,b) \subseteq R \rightarrow R^n$ be a parametrised curve, the speed at the point $\gamma(t)$ is $\dot{\gamma}(t)$. The curve γ is said to be a unit speed curve when $\| \dot{\gamma}(t) \|$ is unit vector.

Proposition 5.1. If $\gamma(s)$ is a unit speed curve, then its curvature k at a point $k(s)$ is defined by the following formula

$$k(s) = \|\gamma''(s)\|$$

Proof: Straightforward by using Equation 8.

Corollary 5.1. Let $\gamma = \gamma(s)$ in R³ be a parametrized curve. Then its curvature is

$$k = \frac{\|\gamma'' \times \gamma'\|}{\|\gamma'\|^3} \tag{19}$$

Proof: By the chain rule, we get

$$\gamma' = \frac{d\gamma}{dt}\frac{dt}{ds}$$

Assume that $\gamma(s)$ is an unite speed curve, yield $k = d^2\gamma\,/dt^2$. Then

$$k = \left\| \frac{d}{dt}\left(\frac{d\gamma/ds}{dt/ds}\right) \right\| = \left\| \frac{\frac{d}{dt}\left(\frac{d\gamma/ds}{dt/ds}\right)}{dt/ds} \right\| = \left\| \frac{\frac{dt}{ds}\frac{d^2\gamma}{ds^2} - \frac{d^2t}{ds^2}\frac{d\gamma}{ds}}{(dt/ds)^3} \right\|$$

Example: consider the helical curve given by:

$$\gamma(s) = a\cos(s)\hat{\imath} + a\sin(s)\hat{\jmath} + b\,s\,\hat{k}$$

with $a\,, b\, > 0$ using formula 2.19, we get the curvature of this helix

$$k = \frac{a}{a^2 + b^2}$$

Now assume that $a = 2\ \ and\ b = 3$ then $k = 2/13$ (exact solution).

5.1. Numerical Approach

Firstly , the space curve $\gamma(s)$ should be inverted point $v_i = (x_i, y_i, z_i)$by evaluating the position vector v_i, at s, where $s = s_1, s_2, s_3, \dots, s_n$ or the curve is itself given as a discrete points $v_1, v_2, v_3, \dots, v_n$ along the curve in the space. In order to find the cur-

vature numerically, we must differentiate function of the curve with respect to the parameter s, i.e.

$$x'(s), y'(s), z'(s), x''(s), y''(s), z''(s)$$

The following formulas are centered finite difference approach

$$x'(s_i) = \frac{x(s_{i+1}) - x(s_i)}{2h} + 0(2) \quad (20)$$

$$x''(s_i) = \frac{x(s_{i+2}) - 2x(s_i) + x(s_{i-1})}{4h^2} + 0(2) \quad (21)$$

and fourth order finite difference approach are used to evaluate the required differentiation.

$$x'(s_{i+2}) = \frac{x(s_{i+1}) - x(s_i)}{12h} + o(4) \quad (22)$$

$$x''(s_{i+2}) = \frac{x(s_i) - 16x(s_{i+1}) + 30x(s_{i+2}) - 16x(s_{i+3})}{-12h^2} + o(4) \quad (23)$$

The second term refers to the error which is increased by approximately 10^n when the step size decreased by a factor of 10.

We will evaluate the curvature of the helix that given in Example 2.5.1 using both approaches for differentiation of the coordinates of the helix $\gamma(s)$ with 101 points.

1. The formula of the centered finite difference method used to differentiate

$$x'(s), y'(s), z'(s), x''(s), y''(s), z''(s),$$

where $x(s) = 2\cos(s)$, $y(s) = 2\sin(s)$, $z(s) = 3s$.

And using the formula 19, the curvature is shown in the following Figure 10.

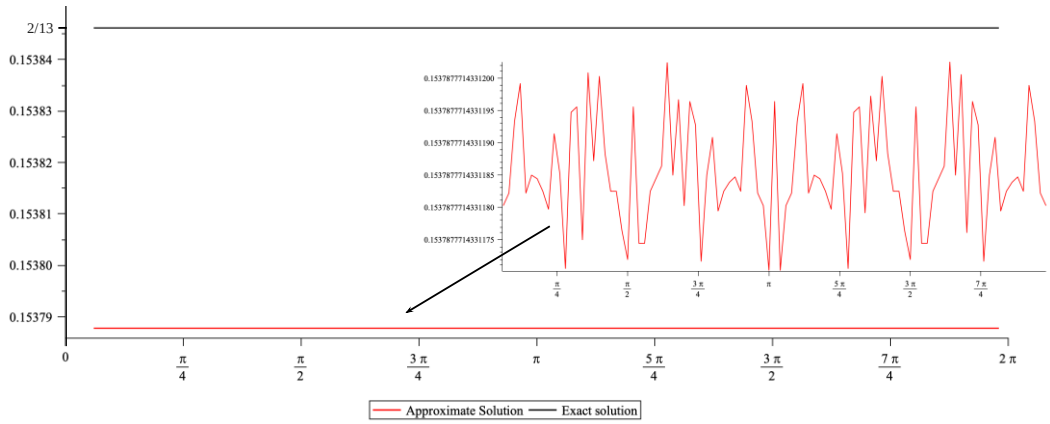

Figure 10 The curvature of the helix using centred finite difference method.

From this figure, we notice that the solution is closed to the exact solution with an absolute error equal to5×10^{-4}.

2. By the same way, we used fourth order finite difference approach, we get the curvature as shown in the Figure 11.

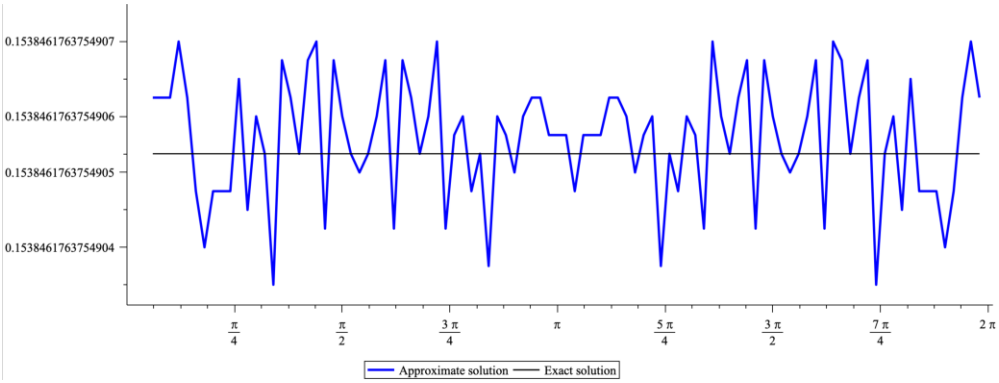

Figure 11 The curvature of the helix using fourth order finite difference method.

Notice that the solution is closed to the exact solution with an absolute error equal to 2.25293×10^{-8}, which indicates that this method is better than the previous one. So, we will be used the fourth order finite difference approach to evaluate the curvature of the field line induced by the magnetic braid.

5.2. Curvature of the field lines of the braid

The same procedure of calculating the curvature of the helix used again to calculate the curvature of some field lines of both the original magnetic braid that defined by Wilmot-Smith and the magnetic braid with four twisting regions. The following figure shows the curvature of some ergodic chaotic field line initiated from same point for both modes. The figure on left shows that the curvature reach approximately 95 when the parameter s = 100, while the other one is approximately 14000. This reflect that the magnetic braid with four toroidal regions have more complexity and can be used as good model in magnetohydrodynamics.

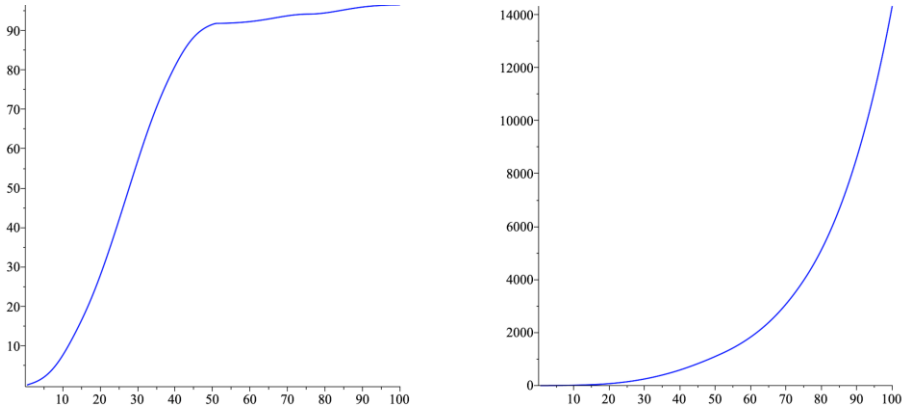

Figure 12 The curvature of a field line starting from the point (1.25, -0.3) in the Wilmot-Smith braid (left), and the curvature of the field line initiated from (1.25, -0.3) in the magnetic braid with four toroidal regions.

6 Conclusion

The curvature of the helix is measured numerically using fourth order finite difference method which is better than centerer finite difference method. Curvature of the field lines of the braid is measured in particular regions in the domain and it shows the ergodic chaotic field line has biggest curvature. The calculation shows that the curvature of the field line of the new-version of the magnetic braid (with for toroidal regions) is much bigger than the curvature of the original model (Wilmot-Smith braid).

7 References

[1] A. R. Yeates, G. Hornig, and A. L. Wilmot-Smith. Topological constraints on magnetic relaxation. Phys. Rev. Lett., 105(8):085002, 2010. doi: 10.1103/PhysRevLett.105.085002.

[2] A. L. Wilmot-Smith and E. R. Priest. Flux tube disconnection - an example of 3d reconnection. Physics of Plasmas, 14(10):102903, 2007.

[3] A. L. Wilmot-Smith, G. Hornig, and D. Pontin. Magnetic braiding and parallel electric fields. Astrophys. J., 696:1339, 2009a.

[4] C. C. Adams, The Knot Book: An Elementary Introduction to the Mathematical Theory of Knots. New York: W. H. Freeman, pp. 132-133, 1994.

[5] Michael R. Allshouse, Jean-Luc Thiffeault, Detecting coherent structures using braids, Physica D Nonlinear Phenomena 241(2) 2007.

[6] Andrew J. Casson, Steven A Bleiler, Automorphisms of Surfaces After Nielsen and Thurston, Cambridge University Press, 1988. ISBN 0-521-34985-0.

[7] Stephen P. Humphries, Generators for the mapping class group, in: Topology of low-dimensional manifolds (Proc. Second Sussex Conf., Chelwood Gate, 1977), pp. 44–47, Lecture Notes in Math., 722, Springer, Berlin, 1979.

[8] W. B. R. Lickorish, A representation of orientable combinatorial 3-manifolds. Ann. of Math. (2) 76 1962 531-540.

[9] W. B. R. Lickorish, A finite set of generators for the homotopy group of a 2-manifold, Proc. Cambridge Philos. Soc. 60 (1964), 769-778

[10] A. L. Wilmot-Smith. The Origin and Dynamic Interaction of Solar magnetic fields. PhD thesis, University of St. Andrews, 2007.

[11] do Carmo and P. Manfredo, Differential Geometry of Curves and Surfaces (revised $\&$ updated 2nd ed.). Mineola, NY: Dover Publications, Inc. pp. 27–28. ISBN 978-0-486-80699-0, 2016.

[12] Kuhnel Wolfgang, Differential Geometry: Curves, Surfaces, Manifolds. Providence: AMS. p. 53. ISBN 0-8218-3988-8, 2005.

[13] M. A. Spivak, Comprehensive introduction to differential geometry, Volumes 1 and 2, Publish or Perish, 1979.

[14] T. Frankel, The geometry of physics: An introduction, 3rd Edition, Cambridge University Press, 2012.

[15] S. Candelaresi, G. Hornig, B. Podger, and D. I. Pontin, Topo- logical Constraints in the Reconnection of Vortex Braids, ArXive, arXiv:1907.11071v2, pp. 1-9, 2021.

Article submitted 16 October 2021. Published as resubmitted by the authors 29 November 2021.